



# Non-fused Phospholes as Fluorescent Probes for Imaging of Lipid Droplets in Living Cells

Elisabet Öberg<sup>†</sup>, Hanna Appelqvist<sup>†</sup> and K. Peter R. Nilsson<sup>\*</sup>

Division of Chemistry, Department of Physics, Chemistry and Biology, Linköping University, Linköping, Sweden

Molecular tools for fluorescent imaging of specific compartments in cells are essential for understanding the function and activity of cells. Here, we report the synthesis of a series of pyridyl- and thienyl-substituted phospholes and the evaluation of these dyes for fluorescent imaging of cells. The thienyl-substituted phospholes proved to be successful for staining of cultured normal and malignant cells due to their fluorescent properties and low toxicity. Co-staining experiments demonstrated that these probes target lipid droplets, which are, lipid-storage organelles found in the cytosol of nearly all cell types. Our findings confirm that thienyl-substituted phospholes can be utilized as fluorescent tools for vital staining of cells, and we foresee that these fluorescent dyes might be used in studies to unravel the roles that lipid droplets play in cellular physiology and in diseases.

**Keywords:** phospholes, fluorescence, cells, imaging, lipid droplets

## OPEN ACCESS

### Edited by:

Andrew Clayton,  
Swinburne University of Technology,  
Australia

### Reviewed by:

Kellie Tuck,  
Monash University, Australia  
George Kokotos,  
National and Kapodistrian University  
of Athens, Greece

### \*Correspondence:

K. Peter R. Nilsson  
petni@ifm.liu.se

<sup>†</sup>These authors have contributed  
equally to this work.

### Specialty section:

This article was submitted to  
Chemical Biology,  
a section of the journal  
Frontiers in Chemistry

**Received:** 10 January 2017

**Accepted:** 06 April 2017

**Published:** 25 April 2017

### Citation:

Öberg E, Appelqvist H and  
Nilsson KPR (2017) Non-fused  
Phospholes as Fluorescent Probes for  
Imaging of Lipid Droplets in Living  
Cells. *Front. Chem.* 5:28.  
doi: 10.3389/fchem.2017.00028

## INTRODUCTION

Fluorescence based cellular imaging is an essential technique for visualizing the localization and the dynamics of cellular compartments and molecular processes (Weijer, 2003; Giepmans et al., 2006; Pittet and Weissleder, 2011; Germain et al., 2012). Hence, the development of fluorescent dyes for optical imaging of distinct cellular components is essential. In this regard, conjugated poly- and oligoelectrolytes (CPEs and COEs), optoelectronic materials normally used in classical organic electronics, have emerged as novel tools for fluorescent imaging of distinct cellular elements (Björk et al., 2007; McRae et al., 2008; Pu et al., 2010; Ding et al., 2011; Pu and Liu, 2011; Feng et al., 2012; Li and Liu, 2012; Cieślár-Pobuda et al., 2014; Gwozdzińska et al., 2014; Magnusson et al., 2015). Due to their electronically delocalized conjugated backbones, CPEs and COEs exhibit intrinsic fluorescent characteristics and offer the opportunity to use a variety of fluorescent imaging methods, as well as different modes of detection, such as excitation- and emission spectra, as well as fluorescent decay (Magnusson et al., 2014). In addition, these fluorescent tools also display rather high photo-bleaching thresholds and stability, two parameters that occasionally limit the effectiveness of conventional fluorescent reporter systems, such as fluorophore labeled antibodies or fluorescent proteins, for fluorescent imaging of cells (Medintz et al., 2005).

From a chemical perspective, the optical and electronic properties of the optoelectronic conjugated materials can be modified by introduction of heteroatoms heavier than carbon, such as sulfur, selenium, or phosphorus, in these systems (Barbarella et al., 2005; Anthony, 2006; Beaujuge and Reynolds, 2010). In this aspect, phosphorus has shown to be especially useful, due to the possibilities to modify the heteroatom through oxidation and metal coordination (Fadhel et al., 2010; Joly et al., 2016; Shameem and Orthaber, 2016). One of the most frequently featured motifs within phosphorus-containing organic conjugated materials is the phosphole moiety.

Phospholes are unsaturated five-membered heterocycles analogous to thiophenes and pyrroles. The 1H-phosphole, i.e., the unsubstituted phosphole (**Figure 1A**), was first characterized in 1983 (Charrier et al., 1983). The motif has since then successfully been incorporated in functional materials e.g., as in thienyl-substituted phospholes (**Figure 1B**). These types of materials have been used in optoelectronic applications such as organic light-emitting diodes (OLEDs), white organic light-emitting diodes (WOLEDs), non-linear optics (NLOs), and solar cells (Crassous and Réau, 2008; Joly et al., 2016; Shameem and Orthaber, 2016). However, in the field of bioimaging, the use of phospholes are relatively scarce and, to the best of our knowledge, there are only two examples to date where benzophospholes (**Figure 1C**) and naphthophospholes (**Figure 1D**) have been used as fluorescent probes. In these systems, the phosphole ring is fused with a phenyl- or naphthyl-ring. These types of probes have been used for imaging of HeLa cells, adipocytes, and preadipocytes (Wang et al., 2015; Yamaguchi et al., 2015). Herein, we synthesized a series of pyridyl- and thienyl-substituted phospholes (**Scheme 1**) and evaluated these compounds as fluorescent tools for fluorescent imaging of cells. The thienyl-substituted phospholes could be used for staining of distinct cellular compartments in living cells without major influence on cell viability or proliferation of the cells. In addition, the staining pattern demonstrated high congruence with Nile Red, a fluorescent stain used to stain lipid droplets (Greenspan et al., 1985), dynamic cytoplasmic compartments that are associated with the etiology of several metabolic disorders such as obesity, diabetes and atherosclerosis (Krahmer et al., 2013). Overall, our studies verified that thienyl-substituted phospholes could be utilized for staining of living cells and we foresee that these dyes might be utilized for organelle specific fluorescence based cellular imaging.

## MATERIALS AND METHODS

### General Procedures

All synthetic manipulations were carried out under inert atmosphere ( $N_2$  or Ar) and under ambient conditions, unless otherwise stated. Chemicals were obtained from Sigma-Aldrich and used as received. THF were dried over Na/Benzophenone or 4 Å molecular sieves.  $^1H$ -NMR and  $^{13}C$ -NMR spectra were recorded on a Varian instrument operating at a proton frequency of 300 MHz in  $CDCl_3$  with or without TMS as internal standard

and water. The spectra were referenced to solvent residual peaks as internal standard and reported in ppm ( $CHCl_3$ :  $\delta_H = 7.26$  ppm,  $\delta_C = 77.0$  ppm).  $^{31}P\{^1H\}$ -NMR measurements were recorded on the same instrument. Column chromatography was performed on silica gel, high purity grade, pore size 60 Å, 230–400 mesh particle size. Filtrations were performed on aluminum oxide, activated basic, Brockmann type I. TLC was performed on silica gel matrix plates with a fluorescent indicator at 254 nm from Fluka.

### Synthesis of 1–3a,b

Octadiynes and phospholes **1–3a,b** were prepared according to literature procedures (Hay et al., 2001; Fadhel et al., 2009) and the NMR assignments of the molecules were in line with these reports (see Supplementary Materials).

### Optical Characterization of the Dyes

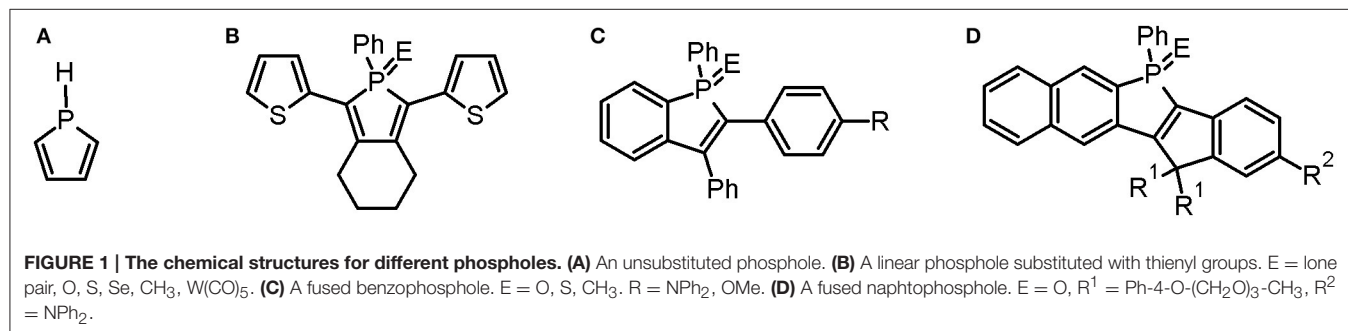
Phospholes **2a,b** and **3a,b** were dissolved in DMSO to a final concentration of 1.5 mM. For the emission spectra in DMSO, 7  $\mu$ l of the stock solution was added to 1000  $\mu$ l of DMSO yielding a final concentration of 10  $\mu$ M. For the phosphate buffer saline pH: 7.4 (PBS) solutions, 7  $\mu$ l of the stock solution was added to 1000  $\mu$ l of PBS, yielding a final concentration of 10  $\mu$ M of the probe and 0.7% DMSO. Emission spectra and excitation spectra were collected using a Hitachi U-1900 Spectrophotometer (Hitachi High-Technologies Corporation, Tokyo, Japan) and a Tecan infinite M1000 Pro (Tecan Group Ltd., Männedorf, Switzerland). A smooth function was applied to the excitation and emission data for noise reduction.

### Cell Lines and Culture Conditions

Normal human skin fibroblasts (AG01518; passages 12–24; Coriell Institute, Camden, NJ, USA) and malignant melanoma cells SK-MEL-28 (HTB-72; ATCC, Manassas, VA, USA) were cultured in Eagle's minimum essential medium (EMEM) GlutaMAX, supplemented with 50 IU/ml penicillin-G, 50  $\mu$ g/ml streptomycin, and 10% fetal bovine serum (all from Gibco, Paisley, UK). Cells were incubated in humidified air with 5%  $CO_2$  at 37°C. The day before experiments, cells were trypsinized and seeded to reach 50% confluence. For microscopic examination, cells were seeded on glass coverslips No 1.0.

### Vital Staining and Fixation of Cells

The cell lines were stained with 10  $\mu$ M of **2a,b** and **3a,b** in complete cell culture media for up to 48 h. In all experiments,



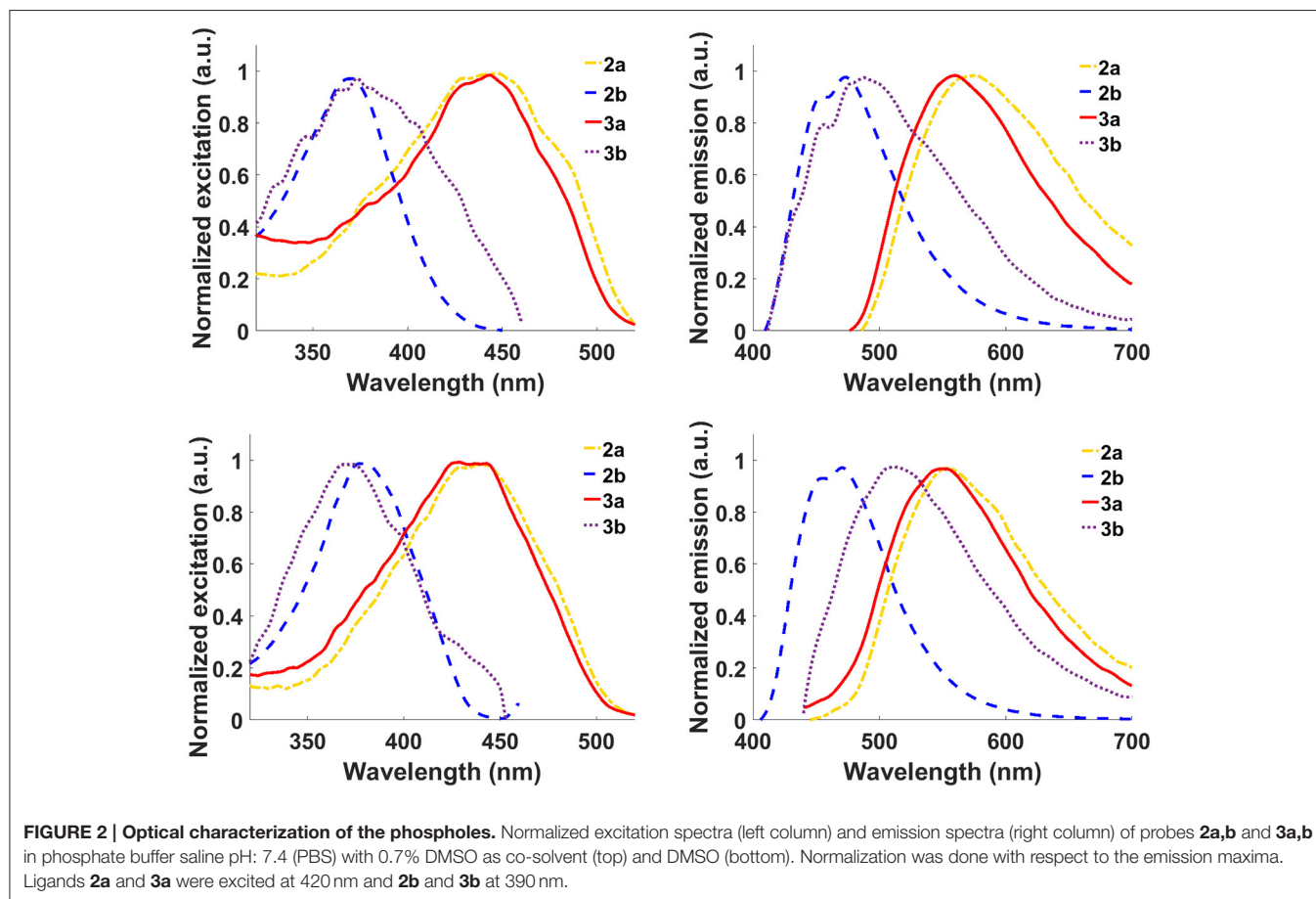
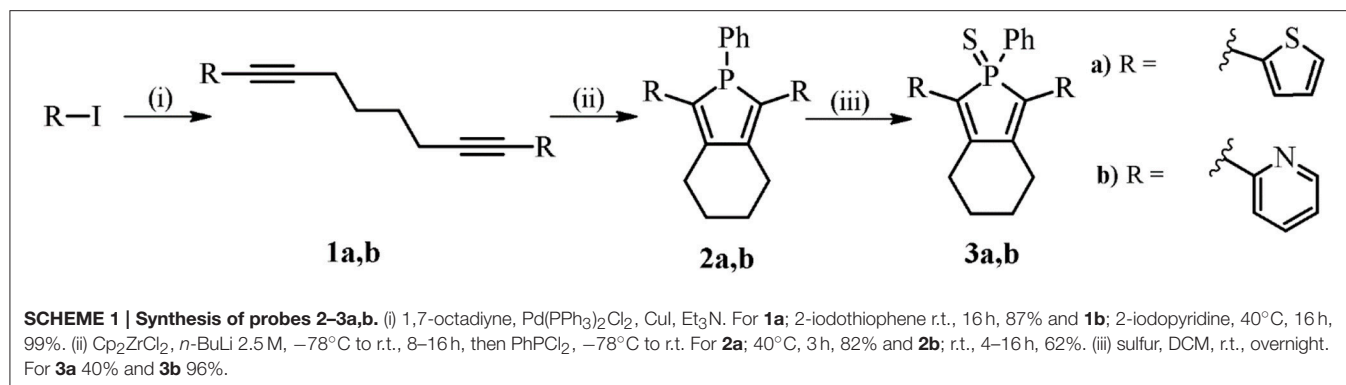
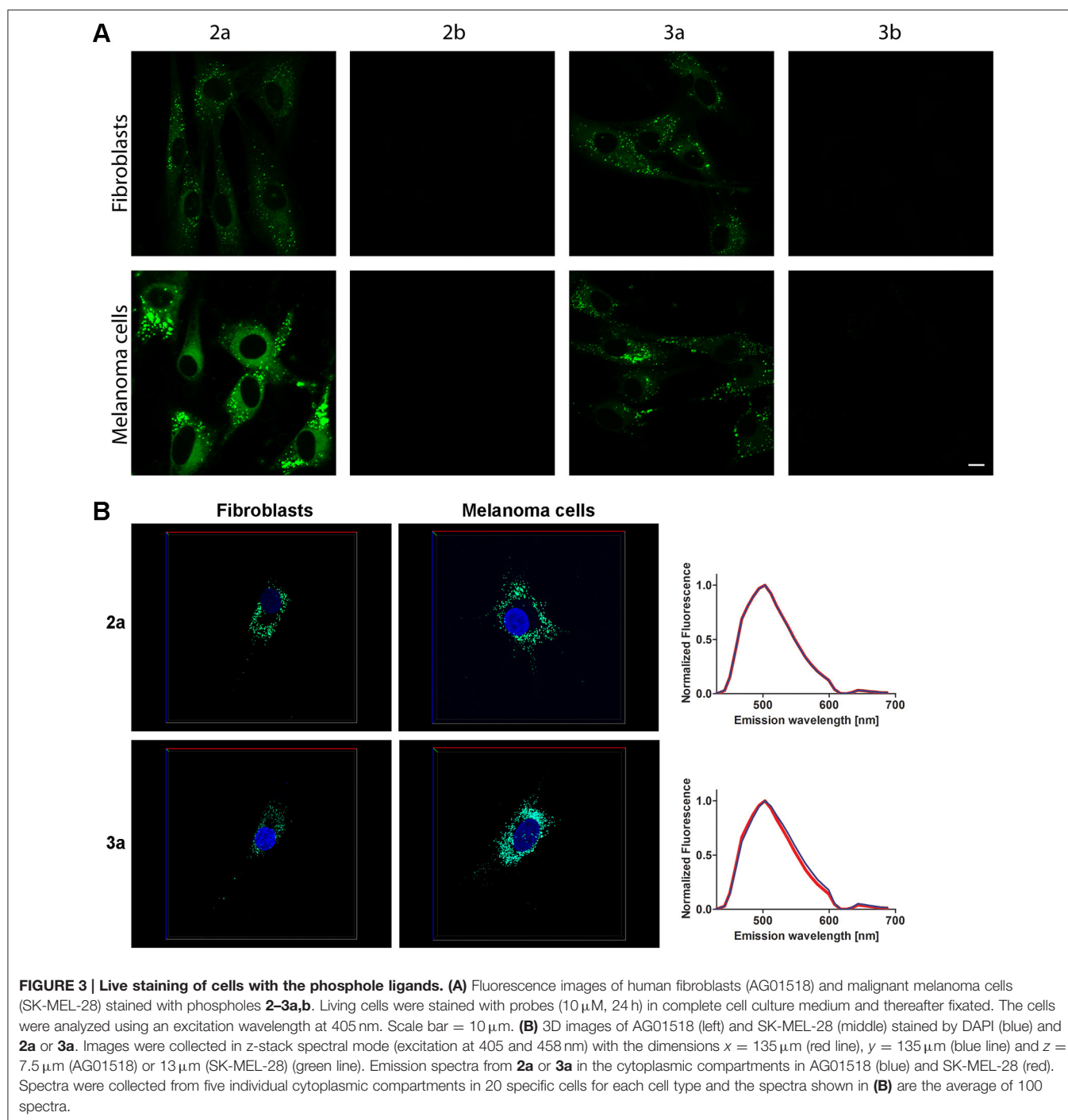


**TABLE 1 | Excitation- and emission maxima of probes 2a,b and 3a,b in PBS<sup>a</sup> and DMSO.**

Probe	Exc <sub>max</sub> PBS <sup>a</sup>	Em <sub>max</sub> PBS <sup>a</sup>	Stoke's shift PBS <sup>a</sup>	Exc <sub>max</sub> DMSO	Em <sub>max</sub> DMSO	Stoke's shift DMSO
2a	446	574	128	439	554	115
2b	371	474	103	377	470	93
3a	443	560	117	429	550	121
3b	374	490	116	374	512	138

<sup>a</sup>PBS with 0.7% DMSO.

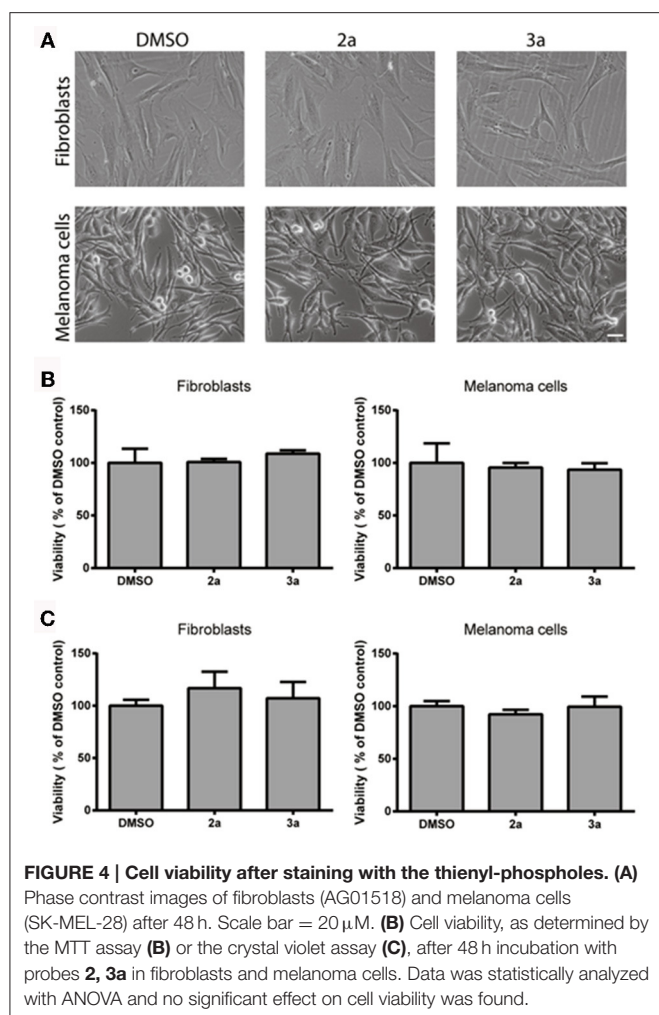


a corresponding DMSO control was run in parallel. For microscopic evaluation, the cells were rinsed three times with PBS, fixed in 4% paraformaldehyde (PFA; 20 min, 4°C) and mounted using Vectashield without or with DAPI (Vector Laboratories, Burlingame, CA, USA) (Williamson and Fennell, 1975) for visualization of cell nuclei.

### Co-staining with Organelle Markers

For staining of mitochondria, probe-stained cells were incubated with MitoTracker Orange CMTMRos (150 nM, 30 min, 37°C;

Molecular Probes, Eugene, OR). Cells were then fixed in 4% PFA (20 min, 4°C). For immunostaining, stained cells were after fixation permeabilized with 0.1% saponin (Sigma-Aldrich) in PBS containing 5% fetal bovine serum (20 min, room temperature) and incubated for 2 h at room temperature with the monoclonal mouse primary antibodies: lysosome-associated membrane protein 2 (LAMP-2, 1:50; Southern Biotech, Birmingham, AL) or early endosomal antigen-1 (EEA-1, 1:400; Sigma-Aldrich). This step was followed by incubation with the appropriate secondary antibodies conjugated to Alexa Fluor 594 (1:400, Molecular



Probes) for 1 h. For staining of lipid droplets fixed cells were stained with 0.1  $\mu$ g/ml Nile Red in 150 mM NaCl, 10 min at room temperature. All incubations were done in the dark. Next, the cells were mounted in Vectashield (Vector Laboratories) and examined with a Zeiss confocal microscope, LSM 780 (Carl Zeiss AG, Germany).

## Fluorescence Microscopy of Stained Cells

For microscopic analysis of the samples, an inverted LSM 780 confocal microscope (Carl Zeiss, Oberkochen, Germany) was used. Phospholes were generally excited at 405 nm. However, when **2a** and **3a** were used together with DAPI the phospholes were excited at 458 nm or 505 nm. DAPI was excited at 405 nm and emission collected at 410–443 nm, while the emission from the probes were collected at 510–749 nm. A plan-Apochromat 633/1.40 Oil DIC 60 X M27 objective was used for all imaging.

## Viability Analysis

The reducing capacity of cell cultures was measured using the 3-(4,5-dimethylthiazol-2-yl)-2,5-diphenyltetrazolium bromide (MTT) reduction assay (Sigma-Aldrich). This method is widely used to assess cytotoxicity and cell viability, and it is currently

thought that the amount of MTT formazan is proportional to the number of living cells (van Meerloo et al., 2011). Cells were incubated with 0.5 mg/ml MTT for 2 h at 37°C. Then, the MTT solution was removed and the formazan product was dissolved in DMSO. The absorbance was measured at 550 nm with a VICTOR™ X Series Multiple Plate Reader (PerkinElmer, Waltham, MA). In addition, cell survival was analyzed using the crystal violet assay. Cells were fixed in 4% PFA (20 min, 4°C), stained with 0.04% crystal violet in 1% ethanol (20 min, room temperature), washed extensively with water and thereafter air-dried. The dye was dissolved in 1% SDS (3 h, rocking, room temperature) and thereafter the absorbance was measured at 550 nm.

## Statistical Analysis

All experiments were repeated four times and the results are presented as the means and standard deviations of independent samples. Data were statistically evaluated using ANOVA.  $P \leq 0.05$  were considered to be significant. All calculations were done using SPSS Statistics 24.

## RESULTS AND DISCUSSION

### Synthesis and Optical Characterization of the Phospholes

For the preparation of the phosphole derivatives, two structural motifs were selected, the thienyl, and the pyridyl unit. Pyridyl-substituted phospholes have started to find their way into biological and medicinal chemistry and the idea was to use phosphole **2b** (Scheme 1) as a reference system since it has shown to have a low toxicity in the human breast cancer cell line MCF-7 (Viry et al., 2008). In addition, the thienyl substituent was chosen in order to have a probe with a more red-shifted spectrum compared to the pyridyl-substituted phosphole (Hay et al., 2001). The synthesis of the phospholes is presented in Scheme 1, and was performed in accordance with established procedures (Hay et al., 2001; Fadhel et al., 2009). Firstly, octadiynes **1a** and **1b** were synthesized through a Sonogashira cross-coupling reaction, with Pd(PPh<sub>3</sub>)<sub>2</sub>Cl<sub>2</sub> and CuI as catalysts in triethyl amine. Secondly, the Fagant-Nugent approach was applied in order to form the phosphole (Fagan and Nugent, 1988; Fagan et al., 1994). In this reaction, a zirconium intermediate is formed, which converts to a phosphole upon addition of *P,P*-dichlorophenylphosphine (Hay et al., 2001; Fadhel et al., 2009). Phospholes **2a,b** were filtered on basic alumina and in contrast to earlier reports, **2a,b** were purified by flash chromatography on silica. This methodology decreased the yield, compared to the earlier reported methods, but was a convenient way to isolate **2a,b** as yellow solids. In the last step, phospholes **2a,b** were oxidized with elemental sulfur and thioxophosphole **3a** was obtained as an orange solid and **3b** as an orange to yellow solid. The structure of the synthesized compounds were confirmed with <sup>1</sup>H-NMR, <sup>13</sup>C-NMR, and <sup>31</sup>P NMR (Supplementary Material).

Next, the optical properties of the probes in different solvents were explored. For cell imaging using phosphole probes, phosphate buffer saline pH: 7.4 (PBS) with DMSO as co-solvent have been employed earlier (Viry et al., 2008; Wang et al.,

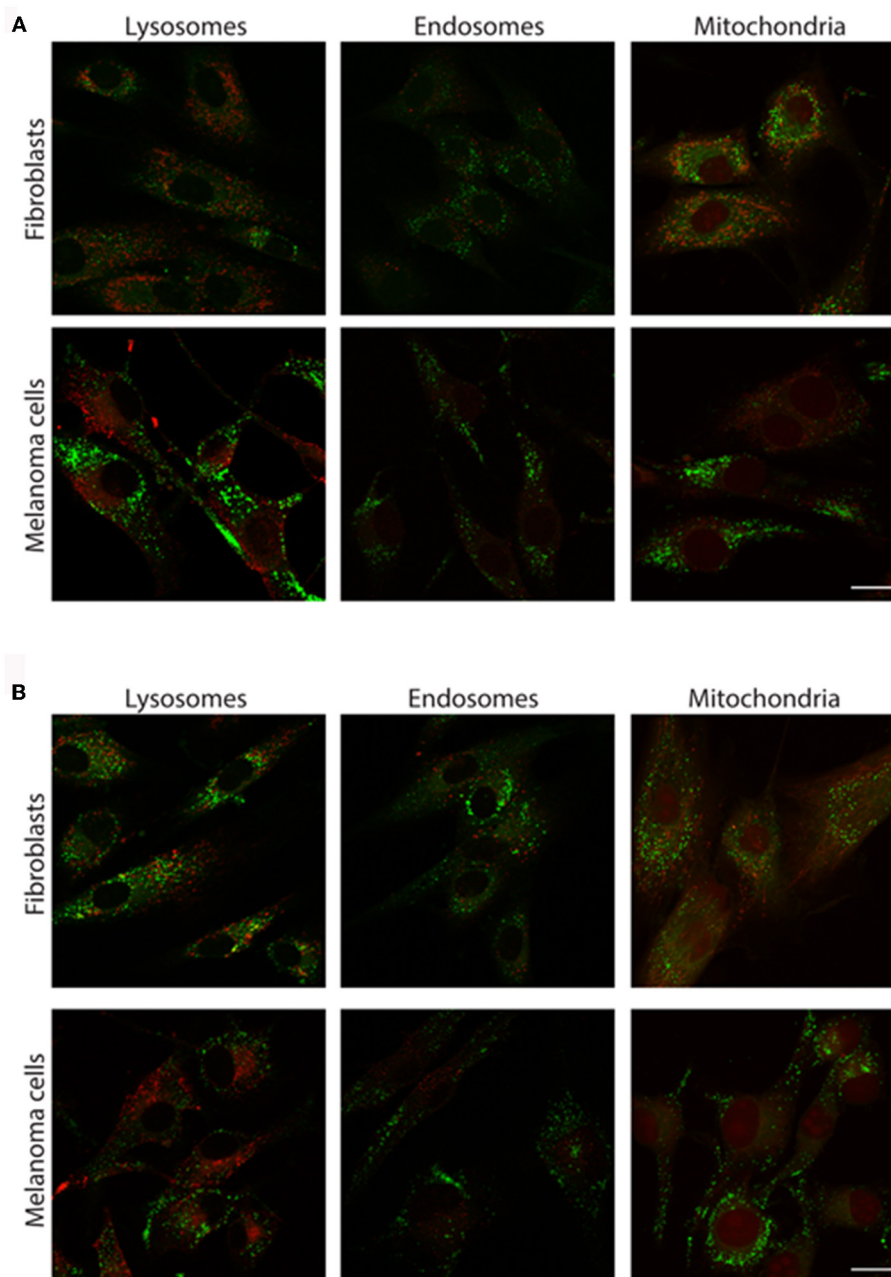
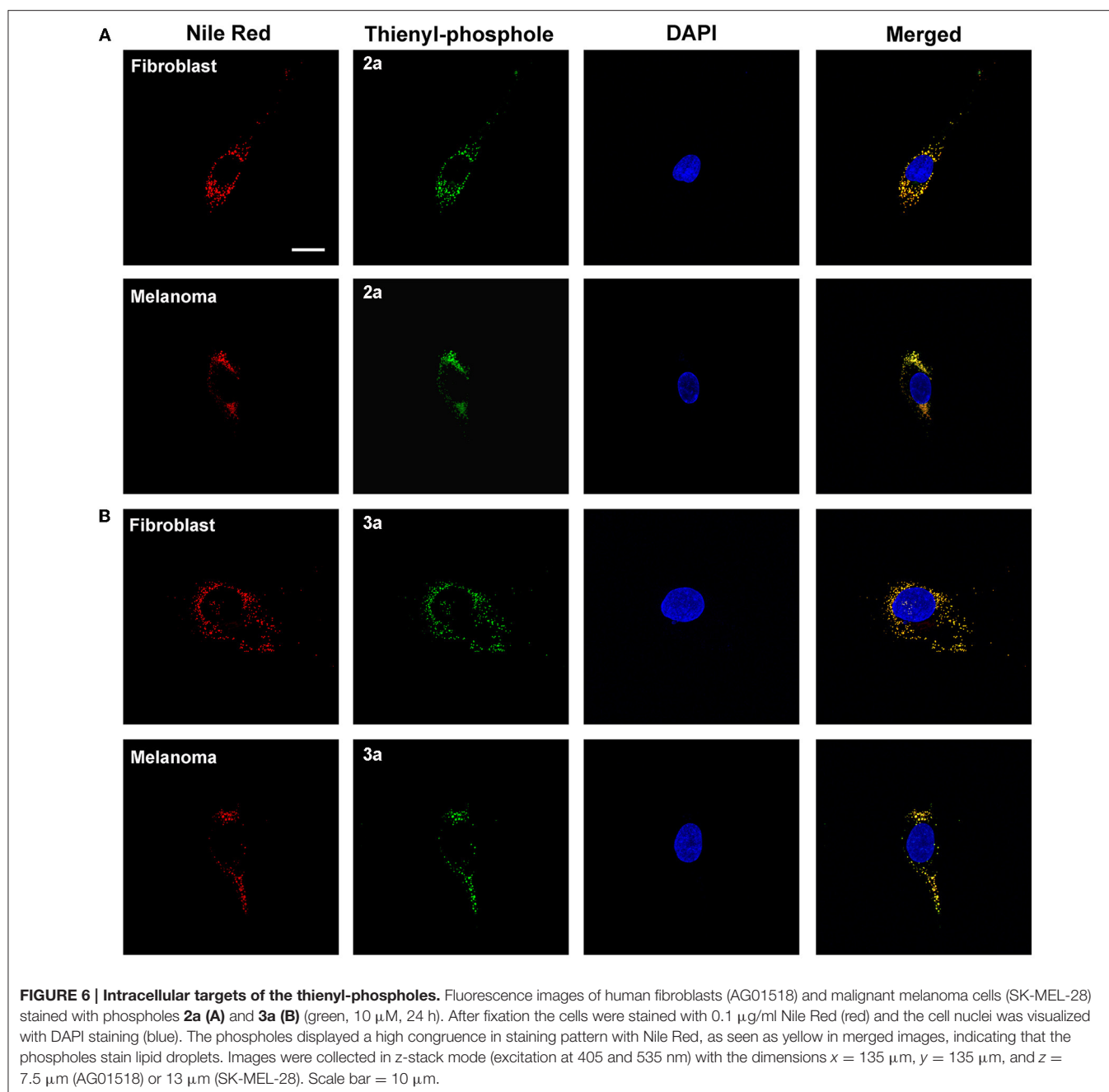


**FIGURE 5 | Costaining of cells with the thienyl-phospholes and markers for intracellular compartments.** Fluorescence images of human fibroblasts (AG01518) and malignant melanoma cells (SK-MEL-28) stained with phospholes **2a** (A) and **3a** (B), seen in green. The cells were co-stained with markers for lysosomes (LAMP-2), early endosomes (EEA-1), and mitochondria (Mitotracker), seen in red. Scalebars = 10  $\mu$ m.

2015). Therefore, the excitation- and emission characteristics of the newly synthesized phospholes were measured both in pure DMSO and in PBS with 0.7% DMSO (PBS/D) as co-solvent. In DMSO, **2b** and **3b** exhibited excitation maxima at 377 and 374 nm, whereas **2a** and **3a** displayed excitation maxima at longer wavelength, 439 and 429 nm, respectively (Figure 2 and Table 1). In addition, **2a** and **3a**, displayed a red-shift of the excitation maxima in PBS/D compared to pure DMSO. The thienyl associated red-shifts were also apparent

when comparing the emission characteristic of the phospholes. In DMSO, **2a** and **3a** exhibited emission maxima at 554 and 550 nm, whereas the pyridyl analogs, **2b** and **3b** showed emission maxima at shorter wavelength, 470 and 512 nm, respectively (Figure 2 and Table 1). Thus, in agreement with the chemical design, introduction of the thienyl substituent to the phosphole induced more red-shifted excitation and emission characteristics compared to the previously reported pyridyl moiety (Hay et al., 2001).



## Staining of Living Cells with the Phospholes

Next, the non-fused phospholes were utilized to stain normal human skin fibroblasts (AG01518) and malignant melanoma cells (SK-MEL-28). Living cells were stained with 10  $\mu$ M phosphole probes in complete cell culture medium for 24 h followed by fixation of the cells with paraformaldehyde. A punctuated intracellular staining pattern was seen with both **2a** and **3a** (Figure 3A). In contrast, the pyridyl-substituted phospholes **2b** and **3b** did not stain the cells to any substantial degree under similar conditions (Figure 3A).

However, with increased gain a punctate staining pattern could be observed for **3b** (data not shown). The lack of fluorescent cell staining when using pyridyl-substituted phospholes have also been observed earlier in a cancer cell line (Viry et al., 2008). Hence, our results verified that thienyl-substituted phospholes had a superior performance regarding fluorescence cell staining compared to the pyridyl-substituted phospholes and that the thienyl substituent was necessary for achieving phosphole based ligands for fluorescent imaging of cells. These probes were therefore chosen for further investigations.

Compounds **2a** and **2b** could also be applied together with a conventional nuclear stain, such as DAPI (Figures 3B,C). As shown in Figure 3, the spectra recorded from the thienyl-substituted phospholes stained compartments were similar for both of the dyes and displayed emission maxima at 505 nm. Thus, the spectra obtained from the thienyl-substituted phospholes in this cellular compartments were strikingly blue-shifted compared to the emission maxima obtained from the dyes in PBS (Figure 2 and Table 1). The blue-shift might indicate that the dyes bind in a cellular compartment having a less polar environment than water, since the emission spectra are blue-shifted for both compound **2a** and **3a** in pure DMSO compared to PBS (Figure 2).

For use as vital cell stain, it is essential that the probes do not interfere with cell viability. Therefore the long-term effect of the probes on the viability of stained cultures was investigated using the MTT assay, in which the capacity of the cells to reduce soluble MTT into formazan is a measure of cell viability (Denizot and Lang, 1986). The morphology of stained cells was similar to controls (with corresponding DMSO concentration; Figure 4A) and no significant effect on cell viability was observed in fibroblast or melanoma cell cultures 48 h after staining with **2a** or **3a** (Figure 4B). The results were verified using the crystal violet assay (Figure 4C) and thus a significant toxic effect of these compounds can be excluded. Overall, the cell staining experiments, as well as the cell viability studies, suggested that thienyl-substituted phospholes can be used as fluorescent tools for live imaging of cells.

## Intracellular Target of the Thienyl-Phospholes

As **2a** and **3a** did not influence cell viability and demonstrated a punctuated intracellular cytoplasmic staining pattern, we continued to investigate the potential cellular targets of the thienyl-substituted phospholes. First the phosphole ligands were tested in combination with different conventional fluorescent markers toward major cellular organelles. However, no co-localization was observed with fluorescent markers toward lysosomes, endosomes, or mitochondria (Figure 5), indicating that the thienyl-substituted phospholes stained a different cytoplasmic compartment than these major cellular organelles.

Small hydrophobic dyes, such as Nile Red (Greenspan et al., 1985), BODIPY dyes (Spandl et al., 2009), fluoranthenes (Goel et al., 2014), monodansylpentane (Chen et al., 2017), azafluorenes, and azafluorenone derivatives (Sharma et al., 2016), have previously been utilized for selective fluorescent staining

of intracellular lipid droplets. Lipid droplets are found in the cytosol of most eukaryotic cells, where they function as energy reservoirs, sources of lipids for membrane biosynthesis and storage sites for lipids (Farese and Walther, 2009; Beller et al., 2010). In addition, lipid droplets have also been shown to be a key cellular organelle in metabolic disorders, such as diabetes and obesity, as well as in cancer and inflammation (Bozza and Viola, 2010; Greenberg et al., 2011). Hence, fluorescent markers identifying these cytoplasmic compartments are of great interest. Interestingly, both **2a** and **3a** showed a high congruence in staining pattern with Nile Red (Figure 6). Thus, these results indicated that the thienyl-substituted phospholes presented herein can be used for fluorescent assessment of lipid droplets.

## CONCLUSIONS

In conclusion, a series of pyridyl- and thienyl-substituted phospholes was synthesized. Fluorescence studies show that the probes exhibit different emission maxima depending on the polarity of the surrounding environment. In addition, this report shows the first example of staining of cultured cells with non-fused phospholes. Thienyl-substituted phospholes **2a** and **3a** show a punctuated staining pattern and co-staining experiments revealed that this pattern is congruent with the staining pattern of Nile Red. Thus, the thienyl-substituted phospholes are therefore potential probes to visualize lipid droplets and for studying the mechanism affecting these structures. We foresee that these fluorescent dyes might aid in studies to unravel the roles that lipid droplets play in cellular physiology and in diseases.

## AUTHOR CONTRIBUTIONS

EÖ, HA, and KPRN designed and performed the experiments, and wrote the manuscript.

## ACKNOWLEDGMENTS

Our work is supported by the Swedish Foundation for Strategic Research.

## SUPPLEMENTARY MATERIAL

The Supplementary Material for this article can be found online at: <http://journal.frontiersin.org/article/10.3389/fchem.2017.00028/full#supplementary-material>

## REFERENCES

- Anthony, J. E. (2006). Functionalized acenes and heteroacenes for organic electronics. *Chem. Rev.* 106, 5028–5048. doi: 10.1021/cr050966z
- Barbarella, G., Melucci, M., and Sotgiu, G. (2005). The versatile thiophene: an overview of recent research on thiophene-based materials. *Adv. Mater.* 17, 1581–1593. doi: 10.1002/adma.200402020
- Beaujuge, P. M., and Reynolds, J. R. (2010). Color control in n-conjugated organic polymers for use in electrochromic devices. *Chem. Rev.* 110, 268–320. doi: 10.1021/cr900129a
- Beller, M., Thiel, K., Thul, P. J., and Jäcke, H. (2010). Lipid droplets: a dynamic organelle moves into focus. *FEBS Lett.* 584, 2176–2182. doi: 10.1016/j.febslet.2010.03.022
- Björk, P., Nilsson, K. P. R., Lenner, L., Kågedal, B., Persson, B., Inganäs, O., et al. (2007). Conjugated polythiophene probes target lysosome-related acidic vacuoles in cultured primary cells. *Mol. Cell. Probes* 21, 329–337. doi: 10.1016/j.mcp.2007.04.005
- Bozza, P. T., and Viola, J. P. (2010). Lipid droplets in inflammation and cancer. *Prostaglandins Leukot. Essent. Fatty Acids* 82, 243–250. doi: 10.1016/j.plefa.2010.02.005



- Charrier, C., Bonnard, H., De Lauzon, G., and Mathey, F. (1983). Proton [1,5] shifts in P-unsubstituted 1H-phospholes. Synthesis and chemistry of 2H-phosphole dimers. *J. Am. Chem. Soc.* 105, 6871–6877. doi: 10.1021/ja00361a022
- Chen, B. H., Yang, H. J., Chou, H. Y., Chen, C. G., and Yang, W. Y. (2017). Staining of lipid droplets with monodansylpentane. *Methods Mol. Biol.* 1560, 231–236. doi: 10.1007/978-1-4939-6788-9\_17
- Ciešlar-Pobuda, A., Bäck, M., Magnusson, K., Jain, M. V., Rafat, M., Ghavami, S., et al. (2014). Cell type related differences in staining with pentameric thiophene derivatives. *Cytometry A* 85, 628–635. doi: 10.1002/cyto.a.22437
- Crassous, J., and Réau, R. (2008).  $\pi$ -Conjugated phosphole derivatives: synthesis, optoelectronic functions and coordination chemistry. *Dalton Trans.* 6865–6876. doi: 10.1039/b810976a
- Denizot, F., and Lang, R. (1986). Rapid colorimetric assay for cell growth and survival. Modifications to the tetrazolium dye procedure giving improved sensitivity and reliability. *J. Immunol. Methods* 89, 271–277. doi: 10.1016/0022-1759(86)90368-6
- Ding, D., Pu, K. Y., Li, K., and Liu, B. (2011). Conjugated oligoelectrolyte-polyhedral oligomeric silsesquioxane loaded pH-responsive nanoparticles for targeted fluorescence imaging of cancer cell nucleus. *Chem. Commun.* 47, 9837–9839. doi: 10.1039/c1cc13237g
- Fadhel, O., Benkö, Z., Gras, M., Deborde, V., Joly, D., Lescop, C., et al. (2010). 3,4-Dithiaphosphole and 3,3',4,4'-tetrathia-1,1'-biphosphole  $\pi$ -conjugated systems: S makes the impact. *Chem. Eur. J.* 16, 11340–11356. doi: 10.1002/chem.201001463
- Fadhel, O., Gras, M., Lemaitre, N., Deborde, V., Hissler, M., Geffroy, B., et al. (2009). Tunable organophosphorus dopants for bright white organic light-emitting diodes with simple structures. *Adv. Mater.* 21, 1261–1265. doi: 10.1002/adma.200801913
- Fagan, P. J., and Nugent, W. A. (1988). Synthesis of main group heterocycles by metallacycle transfer from zirconium. *J. Am. Chem. Soc.* 110, 2310–2312. doi: 10.1021/ja00215a057
- Fagan, P. J., Nugent, W. A., and Calabrese, J. C. (1994). Metallacycle transfer from zirconium to main group elements: a versatile synthesis of heterocycles. *J. Am. Chem. Soc.* 116, 1880–1889. doi: 10.1021/ja00084a031
- Farese, R. V., and Walther, T. C. (2009). Lipid droplets finally get a little R-E-S-P-E-C-T. *Cell* 25, 855–860. doi: 10.1016/j.cell.2009.11.005
- Feng, G., Ding, D., and Liu, B. (2012). Fluorescence bioimaging with conjugated polyelectrolytes. *Nanoscale* 4, 6150–6165. doi: 10.1039/C2NR31392H
- Germain, R. N., Robey, E. A., and Cahalan, M. D. (2012). A decade of imaging cellular motility and interaction dynamics in the immune system. *Science* 336, 1676–1681. doi: 10.1126/science.1221063
- Giepmans, B. N., Adams, S. R., Ellisman, M. H., and Tsien, R. Y. (2006). The fluorescent toolbox for assessing protein location and function. *Science* 312, 217–224. doi: 10.1126/science.1124618
- Goel, A., Sharma, A., Kathuria, M., Bhattacharjee, A., Verma, A., Mishra, P. R., et al. (2014). New fluoranthene FLUN-550 as a fluorescent probe for selective staining and quantification of intracellular lipid droplets. *Org. Lett.* 16, 756–759. doi: 10.1021/ol403470d
- Greenberg, A. S., Coleman, R. A., Kraemer, F. B., McManaman, J. L., Obin, M. S., Puri, V., et al. (2011). The role of lipid droplets in metabolic disease in rodents and humans. *J. Clin. Invest.* 121, 2102–2110. doi: 10.1172/JCI46069
- Greenspan, P., Mayer, E. P., and Fowles, S. D. (1985). Nile red: a selective fluorescent stain for intracellular lipid droplets. *J. Cell Biol.* 100, 965–973.
- Gwozdzińska, P., Pawłowska, R., Milczarek, J., Garner, L. E., Thomas, A. W., Bazan, G. C., et al. (2014). Phenylenevinylene conjugated oligoelectrolytes as fluorescent dyes for mammalian cell imaging. *Chem. Commun.* 50, 14859–14861. doi: 10.1039/c4cc06478j
- Hay, C., Hissler, M., Fischmeister, C., Rault-Berthelot, J., Toupet, L., Nyulászi, L., et al. (2001). Phosphole-containing  $\pi$ -conjugated systems: from model molecules to polymer films on electrodes. *Chem. Euro. J.* 7, 4222–4236. doi: 10.1002/1521-3765(20011001)7:19<4222::AID-CHEM4222>3.0.CO;2-3
- Joly, D., Bouit, P. A., and Hissler, M. (2016). Organophosphorus derivatives for electronic devices. *J. Mater. Chem. C* 4, 3686–3698. doi: 10.1039/C6TC00590J
- Krahmer, N., Farese, R. V. Jr., and Walther, T. C. (2013). Balancing the fat: lipid droplets and human disease. *EMBO Mol. Med.* 5, 973–983. doi: 10.1002/emmm.201100671
- Li, K., and Liu, B. (2012). Polymer encapsulated conjugated polymer nanoparticles for fluorescence bioimaging. *J. Mater. Chem.* 22, 1257–1264. doi: 10.1039/C1JM14397B
- Magnusson, K., Appelqvist, H., Ciešlar-Pobuda, A., Wiggenius, J., Karlsson, T., Los, M. J., et al. (2015). Differential vital staining of normal fibroblasts and melanoma cells by an anionic conjugated polyelectrolyte. *Cytometry A* 87, 262–272. doi: 10.1002/cyto.a.22627
- Magnusson, K., Simon, R., Sjölander, D., Sigurdson, C. J., Hammarström, P., and Nilsson, K. P. R. (2014). Multimodal fluorescence microscopy of prion strain specific PrP deposits stained by thiophene-based amyloid ligands. *Prion* 8, 319–329. doi: 10.4161/pri.29239
- McRae, R. L., Phillips, R. L., Kim, I.-B., Bunz, U. H. F., and Fahrni, C. J. (2008). Molecular recognition based on low-affinity polyvalent interactions: selective binding of a carboxylated polymer to fibronectin fibrils of live fibroblast cells. *J. Am. Chem. Soc.* 130, 7851–7853. doi: 10.1021/ja8007402
- Medintz, I. L., Uyeda, H. T., Goldman, E. R., and Mattoussi, H. (2005). Quantum dot bioconjugates for imaging, labelling and sensing. *Nat. Mater.* 4, 435–446. doi: 10.1038/nmat1390
- Pittig, M. J., and Weissleder, R. (2011). Intravital imaging. *Cell* 147, 983–991. doi: 10.1016/j.cell.2011.11.004
- Pu, K. Y., Li, K., Zhang, X. H., and Liu, B. (2010). Conjugated oligoelectrolyte harnessed polyhedral oligomeric silsesquioxane as light-up hybrid nanodot for two-photon fluorescence imaging of cellular nucleus. *Adv. Mater.* 22, 4186–4189. doi: 10.1002/adma.201001544
- Pu, K. Y., and Liu, B. (2011). Fluorescent conjugated polyelectrolytes for bioimaging. *Adv. Funct. Mater.* 21, 3408–3423. doi: 10.1002/adfm.201101153
- Shameem, M. A., and Orthaber, A. (2016). Organophosphorus compounds in organic electronics. *Chem. Eur. J.* 22, 10718–10735. doi: 10.1002/chem.201600005
- Sharma, A., Umar, S., Kar, P., Singh, K., Sachdev, M., and Goel, A. (2016). A new type of biocompatible fluorescent probe AFN for fixed and live cell imaging of intracellular lipid droplets. *Analyst* 141, 137–143. doi: 10.1039/c5an01623a
- Spandl, J., White, D. J., Pechl, J., and Thiele, C. (2009). Live cell multicolor imaging of lipid droplets with a new dye, LD540. *Traffic* 10, 1579–1584. doi: 10.1111/j.1600-0854.2009.00980.x
- van Meerloo, J., Kaspers, G. J. L., and Cloos, J. (2011). Cell sensitivity assays: the MTT assay. *Methods Mol. Biol.* 731, 237–245. doi: 10.1007/978-1-61779-080-5\_20
- Viry, E., Battaglia, E., Deborde, V., Müller, T., Réau, R., Davioud-Charvet, E., et al. (2008). A sugar-modified phosphole gold complex with antiproliferative properties acting as a thioredoxin reductase inhibitor in MCF-7 Cells. *Chem. Med. Chem.* 3, 1667–1670. doi: 10.1002/cmdc.200800210
- Wang, C., Fukazawa, A., Taki, M., Sato, Y., Higashiyama, T., and Yamaguchi, S. (2015). A phosphole oxide based fluorescent dye with exceptional resistance to photobleaching: a practical tool for continuous imaging in sted microscopy. *Angew. Chem. Int. Ed. Engl.* 54, 15213–15217. doi: 10.1002/anie.201507939
- Weijer, C. J. (2003). Visualizing signals moving in cells. *Science* 300, 96–100. doi: 10.1126/science.1082830
- Williamson, D. H., and Fennell, D. J. (1975). The use of fluorescent DNA-binding agent for detecting and separating yeast mitochondrial DNA. *Methods Cell Biol.* 12, 335–351.
- Yamaguchi, E., Wang, C., Fukazawa, A., Taki, M., Sato, Y., Sasaki, T., et al. (2015). Environment-sensitive fluorescent probe: a benzophosphole oxide with an electron-donating substituent. *Angew. Chem. Int. Ed. Engl.* 54, 4539–4543. doi: 10.1002/anie.201500229

**Conflict of Interest Statement:** The authors declare that the research was conducted in the absence of any commercial or financial relationships that could be construed as a potential conflict of interest.

Copyright © 2017 Öberg, Appelqvist and Nilsson. This is an open-access article distributed under the terms of the Creative Commons Attribution License (CC BY). The use, distribution or reproduction in other forums is permitted, provided the original author(s) or licensor are credited and that the original publication in this journal is cited, in accordance with accepted academic practice. No use, distribution or reproduction is permitted which does not comply with these terms.